Four distributed feedback laser array integrated with multimode-interference and semiconductor optical amplifier*

Ma Li(马 丽)[a)b)], Zhu Hong-Liang(朱洪亮)[a)†], Liang Song(梁 松)[a)], Zhao Ling-Juan(赵玲娟)[a)], and Chen Ming-Hua(陈明华)[b)]

[a)] *Key Laboratory of Semiconductor Materials Science, Institute of Semiconductors, Chinese Academy of Sciences, Beijing* 100083, *China*
[b)] *Department of Electronic Engineering, Tsinghua University, Beijing* 100084, *China*

(Received 6 September 2012; revised manuscript received 19 November 2012)

Monolithic integration of four 1.55-μm-range InGaAsP/InP distributed feedback (DFB) lasers using varied ridge width with a 4×1-multimode-interference (MMI) optical combiner and a semiconductor optical amplifier (SOA) is demonstrated. The average output power and the threshold current are 1.8 mW and 35 mA, respectively, when the injection current of the SOA is 100 mA, with a side mode suppression ratio (SMSR) exceeding 40 dB. The four channels have a 1-nm average channel spacing and can operate separately or simultaneously.

Keywords: distributed feedback laser array, varied width ridge, monolithic integration, butt joint

PACS: 42.82.Gw, 42.55.Px, 42.82.Cr **DOI:** 10.1088/1674-1056/22/5/054211

1. Introduction

Dense wavelength division multiplexing (DWDM) channel number increases ceaselessly due to the rapid development of demand for internet data communication. Multi-wavelength light sources are now key components in DWDM optical transmission systems and are indispensable in future photonic networks.[1] Several types of multi-wavelength laser sources have been reported: the distributed Bragg reflector (DBR) laser array,[2,3] the distributed feedback (DFB) laser array,[4,5] and integrated devices[6] with integrated multimode interference couplers and semiconductor optical amplifier s.[7,8] DFB laser diode (LD) arrays are widely used for their stable and highly reliable single-mode operation.[9,10] However, the grating of the DFB laser is usually fabricated by electron-beam (EB) lithography to form different wavelengths. This method is time-consuming, costly, and unsuitable for mass production. Holographic exposure is a simple method to fabricate grating, but it needs to introduce sampling grating[11] or reconstruction-equivalent-chirp grating technology to obtain the different wavelength channels. Furthermore, it reduces the side mode suppression ratio (SMSR) for its side mode sampling.

In this paper, a four channel DFB laser array is proposed and demonstrated by varying the width of the ridge of the waveguide. The effective index of the waveguide can be changed by varying the width of the ridge.[12] Therefore, simple holographic lithography and orderly change of the ridge width can be used to realize a different wavelength for each channel. Without additional process steps, this method also does not reduce the SMSR. Using this technique, combined with active/passive butt-joint coupling technology, a monolithic integrated device including a four channel DFB laser array, multimode-interference (MMI), and semiconductor optical amplifier (SOA) is fabricated. The lasing wavelength is 1.55-μm range and the interval between adjacent channels is about 1nm.

2. Design and fabrication

Figure 1 shows the schematic structure of the four channel multi-wavelength DFB laser array (LD1, LD2, LD3, and LD4). The length of the laser and the SOA are 690 μm and 600 μm, respectively. The separation between two DFB lasers is 100 μm. The width and length of the MMI coupler are 24 μm and 310 μm, respectively.

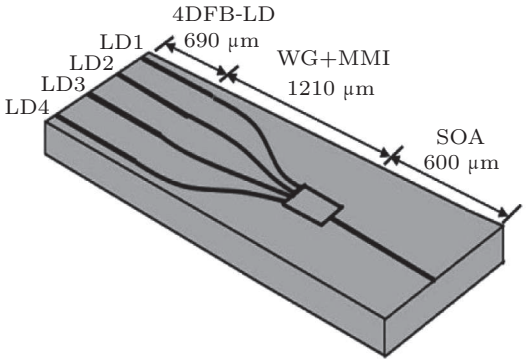


Fig. 1. Schematic structure of the DFB laser array fabricated by using the varied width ridge technique.

For the fabrication of the device, first, an active multi-quantum well (MQW) structure was grown over the entire

*Project supported by the National High Technology Research and Pevelopment Program of China (Grant Nos. 2011AA010303 and 2012AA012203), the National Basic Research Program of China (Grant No. 2011CB301702), and the National Natural Science Foundation of China (Grant Nos. 61021003 and 61090392).

†Corresponding author. E-mail: zhuhl@red.semi.ac.cn

© 2013 Chinese Physical Society and IOP Publishing Ltd

wafer by metal-organic chemical vapor deposition (MOCVD), consisting of 6 compressively strained quantum wells and 5 tensely strained barriers. The MQW material in the passive region was selectively etched by $3H_2SO_4$:H_2O_2:H_2O wet-etching solution. Then a 300-nm InGaAsP waveguide layer with a 1300-nm emission wavelength was grown in a second MOCVD run. After uniform grating was formed in the DFB laser region by holographic exposure, a p-type overcladding and a cap layer were grown on the wafer.

A shallow-ridge waveguide was used for the DFB laser and SOA, while a deep-ridge waveguide was used for the passive waveguide to reduce the size of the device. The ridge widths of the four channels were designed to be 2 μm, 2.3 μm, 2.6 μm, and 3 μm, respectively. The shallow-ridge waveguide was formed by a CH_4:H_2:Ar reactive ion etching (RIE) dry-etching process followed by a short-time wet-etching step, which was stopped at the grating layer. The 250-nm InGaAs contact layer in the passive region was removed by wet-etching to reduce the absorption loss. Finally, Ti/Au p-type and evaporated Au/Ge/Ni n-type electrical contacts were formed. All output facets of the device structure were formed by cleaving without additional dielectric coating.

3. Device characters

The conditions of both wet-etching and MOCVD growth were carefully optimized to obtain a good butt-joint interface between the LD active MQW and the passive waveguide layer. An SEM picture of a cross section of the butt-joint interface between the active MQWs and the passive waveguide is shown in Fig. 2(a). As can be seen, a good butt-joint quality was obtained, as no voids were revealed. Figure 2(b) shows the photoluminescence spectra of the active and passive regions. In order to reduce reflectivity from the MMI coupler and improve the light uniformity into the MMI coupler, waveguides with tapered regions were used,[13] which was 50-μm-long with the width changing from 4 μm to 3 μm, as shown in Fig. 2(c). The fabricated device was mounted onto a Cu heat sink, set at 25 °C, for characterization. Typical light output–current (L–I) characteristics of the lasers with or without the MMI couplers (the MMI is cleaved from the laser with the butt-joint interface) are shown in Fig. 3. As can be seen, at 100-mA injection current, the output power with and without the MMI coupler is 9.3673 mW and 2.1315 mW, respectively. The power loss resulting from the integration of the MMI is then calculated to be 6.429 dB. Considering the 6-dB power loss of a 1×4 MMI, the combined losses resulting from the butt-joint interface, the scattering from the waveguide side walls and the material defects, and the absorption of waveguide materials are as low as 0.429 dB, which results from our optimized experimental conditions.

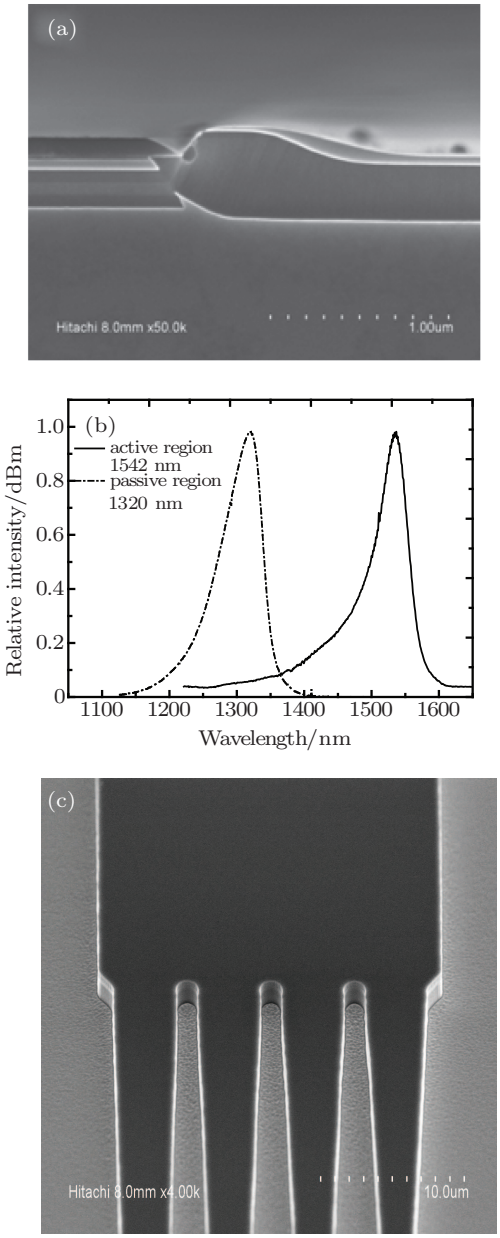


Fig. 2. (a) SEM picture of the butt-joint interface, (b) Photoluminescence spectra of the active and passive regions, and (c) SEM picture of the MMI coupler and tapered waveguides.

The lasing spectra of the device when $I_{DFB} = 50$ mA are shown in Fig. 4 and have an SMSR greater than 40 dB. The lasing wavelengths of the four channels are 1549.965 nm, 1551.105 nm, 1552.255 nm, and 1553.015 nm, respectively. The wavelength spacing between two adjacent channels are 1.14 nm, 1.15 nm, and 0.76 nm, which are not equal. This is because that the effective index of the lasers are not linearly varied with the ridge width. An equal wavelength spacing can be obtained by increasing the ridge width nonlinearly.

Figure 5 shows the L–I curves of a single channel (channel 1) when the injection current of the SOA is 80 mA, 100 mA, 120 mA, and 150 mA, respectively. The output power is increased from 2.27 mW to 4.25 mW (nearly doubled) when the current of the SOA is changed from 80 mA to 150 mA.

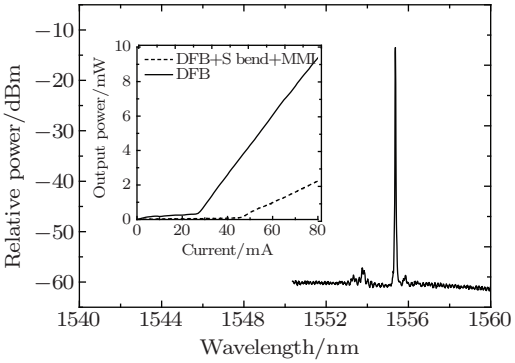


Fig. 3. Typical lasing spectrum of the integrated device. Inset shows *L–I* characteristics of 1900-μm-long DFB-S bend-MMI device and 690-μm-long DFB LD, without waveguide section.

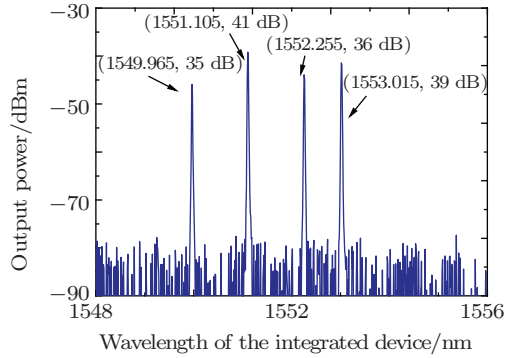


Fig. 4. (color online) Lasing spectra of the integrated device from SOA facet ($I_{DFB} = I_{SOA} = 50$ mA).

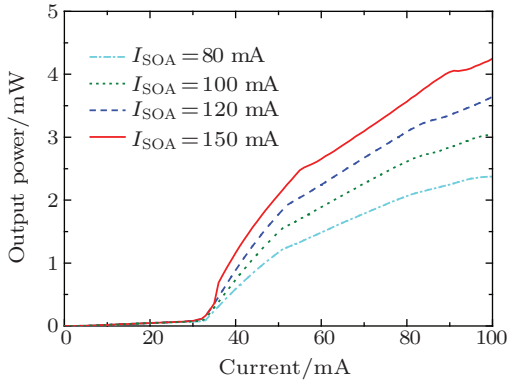


Fig. 5. (color online) Single channel *L–I* characteristics when the SOA injects different currents.

There is a kink characteristic in the light *L–I* curve of the DFB lasers. The mechanism of such a kink is still unclear. Putting a high-reflection coating on the rear of the laser diodes and an antireflection coating on the front of the SOA may avoid the kink.

Figure 6 shows the four channels (CH1, CH2, CH3, and CH4) output power versus the SOA current when the injection current of the four DFB LD are 70 mA. It can be seen that for all the channels, the output power of each of the integrated devices is greater than 4.3 mW when the current of the SOA is 250 mA.

When used in DWDM systems, all the DFB-LDs in a laser array work simultaneously and the output lights must match a series of wavelengths that are typically uniformly spaced. By varying the ridge width as in this work, lasers with roughly uniform channel spacing can be obtained. Fine tuning of laser wavelength is usually needed to align the emission of the array to a specific grid. Thermal tuning of laser wavelength is a simple technique and thus is widely used. It is desirable that wavelength shift occurs only in the heated laser element. Thermal crosstalk, however, inevitably shifts the wavelength of nearby lasers. In order to study the thermal crosstalk among lasers in a laser array, the wavelength shift of LD4 was measured when its bias current was constant at 50 mA, while the bias currents of LD1, LD2, and LD3 are changed in a range from 0 mA to 100 mA, as shown in Fig. 7.

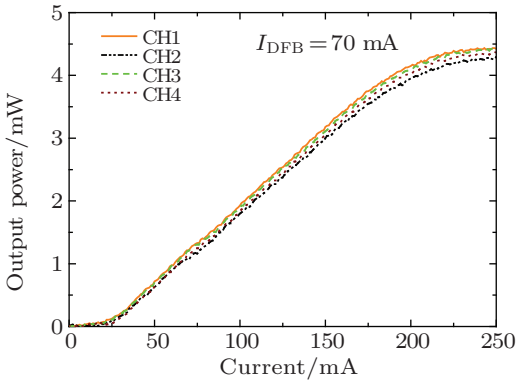


Fig. 6. (color online) Output power as a function of SOA injection current when $I_{DFB} = 70$ mA.

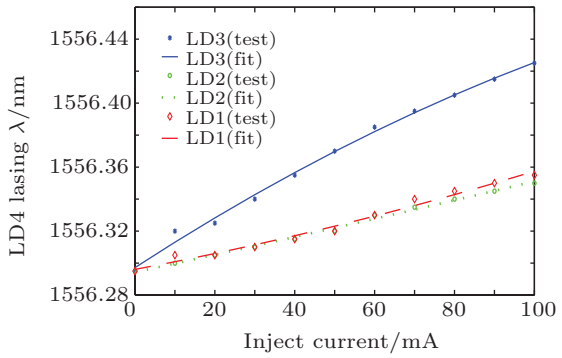


Fig. 7. (color online) Wavelength shift caused by thermal crosstalk of DFB-LD.

Therefore, low-crosstalk characteristics are important. Widening channel spacing can reduce the effects of the neighboring channels. On the other hand, narrow channel spacing is very effective for minimizing the size of a transmitter, which consists of a DFB-LD array and a combiner.[14]

4. Conclusion

A monolithic integration of four 1.55-μm-range InGaAsP/InP distributed feedback lasers with a 4×1-MMI optical combiner and an SOA using a varied width ridge method is proposed and demonstrated. The typical threshold current is 35 mA and the average output power for each channel is

1.8 mW when the current of the LD and the SOA are both 100 mA. The lasing wavelength is in the 1.55-μm range. The four channels can operate separately or simultaneously. This device is promising for wide use in compact transmitter modules for 10-Gb/s four-channel DWDM network systems.

References

[1] Yashiki K, Sato K, Morimoto T, Sudo S, Naniwae K, Ae S, Shiba K, Suzuki N, Sasaki T and Kudo K 2004 *IEEE Photon. Technol. Lett.* **16** 1619

[2] Matsuo S, Kakitsuka T, Segawa T, Sato R, Shibata Y, Takahashi R, Oohashi H and Yasaka H 2008 *IEEE Photon. Technol. Lett.* **20** 1494

[3] Fujiwara N, Kakitsuka T, Ishikawa M, Kano F, Okamoto H, Kawaguchi Y, Kondo Y, Yoshikuni Y and Tohmori Y 2003 *IEEE J. Select. Topics Quantum Electron.* **9** 1132

[4] Zhu H L, Xu X D, Wang H, Kong D H, Liang S, Wang B J, Zhao L J and Wang W 2010 *IEEE Photon. Technol. Lett.* **22** 353

[5] Chen X F, Liu W, An J M, Liu Y, Xu K, Wang X, Liu J G, Ji Y F and Zhu N H 2011 *Chin. Sci. Bull.* **56** 3064

[6] Liao Z Y, Yang H and Wang W 2008 *Chin. Phy. B* **17** 2557

[7] Nunoya N, Ishii H, Kawaguchi Y, Iga R, Sato T, Fujiwara N and Oohashi H 2011 *IEEE J. Select. Topics Quantum Electron.* **17** 1505

[8] Nunoya N, Ishii H, Kawaguchi Y, Kondo Y and Oohashi H 2008 *Electron. Lett.* **44** 205

[9] Xie H Y, Wang L, Zhao L J, Zhu H L and Wang W 2007 *Chin. Phys.* **16** 1459

[10] Wang C L, Wu J and Lin J T 2003 *Chin. Phys.* **12** 528

[11] Wang H, Zhu H L, Jia L H, Chen X F, Kong D H, Wang L S, Zhang W, Zhao L J and Wang W 2009 *Chin. Phys. B* **18** 2868

[12] Kong D H, Zhu H L, Liang S, Zhao X F, Lou C Y, Wang L, Wang B J and Zhao L J 2010 *Opt. Commun.* **283** 3970

[13] Ma L, Zhu H L and Chen M H 2012 *Proceedings of SPIE*, January 23–25, 2012, San Francisco, CA

[14] Tsuruoka K, Kobayashi R, Ohsawa Y, Tsukuda T, Kato T, Sasaki T and Nakamura T 2005 *IEEE J. Quantum Electron.* **11** 1169